Multifunctional Stable and pH-Responsive Polymer Vesicles Formed by Heterofunctional Triblock Copolymer for Targeted Anticancer Drug Delivery and Ultrasensitive MR Imaging

Xiaoqiang Yang,[†] Jamison J. Grailer,[‡] Ian J. Rowland,[§] Alireza Javadi,[⊥] Samuel A. Hurley,[§] Vyara Z. Matson,[‡] Douglas A. Steeber,[‡] and Shaoqin Gong[⊥,*]

[†]Department of Mechanical Engineering and [‡]Department of Biological Sciences, University of Wisconsin—Milwaukee, Milwaukee, Wisconsin 53211, United States and [§]Department of Medical Physics and [⊥]Department of Biomedical Engineering and Wisconsin Institute for Discovery, University of Wisconsin—Madison, Madison, Wisconsin 53706, United States

ABSTRACT A multifunctional stable and pH-responsive polymer vesicle nanocarrier system was developed for combined tumor-targeted delivery of an anticancer drug and superparamagnetic iron oxide (SPIO) nanoparticles (NPs). These multifunctional polymer vesicles were formed by heterofunctional amphiphilic triblock copolymers, that is, R (folate (FA) or methoxy)-poly(ethylene glycol)(M_w:5000)-poly(glutamate hydrozone doxorubicin)-poly(ethylene glycol) (M_w: 2000)-acrylate (*i.e.*, R (FA or methoxy)-PEG_{114}-P(Glu-Hyd-DOX)-PEG_{46}-acrylate). The amphiphilic triblock copolymers can self-assemble into stable vesicles in aqueous solution. It was found that the long PEG segments were mostly segregated into the outer hydrophilic PEG layers of the vesicles, thereby providing active tumor targeting *via* FA, while the short PEG segments were mostly segregated into the inner hydrophilic PEG layer of the vesicles, thereby making it possible to cross-link the inner PEG layer *via* the acrylate groups for enhanced *in vivo* stability. The therapeutic drug, DOX, was conjugated onto the polyglutamate segment, which formed the hydrophobic membrane of the vesicles using a pH-sensitive hydrazone bond to achieve pH-responsive drug release, while the hydrophilic SPIO NPs were encapsulated into the aqueous core of the stable vesicles, allowing for ultrasensitive magnetic resonance imaging (MRI) detection. The SPIO/DOX-loaded vesicles demonstrated a much higher r_2 relaxivity value than Feridex, a commercially available SPIO-based T_2 contrast agent, which was attributed to the high SPIO NPs loading level and the SPIO clustering effect in the aqueous core of the vesicles. Results from flow cytometry and confocal laser scanning microscopy (CLSM) analysis showed that FA-conjugated vesicles exhibited higher cellular uptake than FA-free vesicles which also led to higher cytotoxicity. Thus, these tumor-targeting multifunctional SPIO/DOX-loaded vesicles will provide excellent *in vivo* stability, pH-controlled drug release, as well as enhanced MRI contrast, thereby making targeted cancer therapy and diagnosis possible.

KEYWORDS: polymer vesicles · nanoparticles · drug delivery · iron oxide · cancer therapy · magnetic resonance imaging · triblock copolymers

Multifunctional nanocarriers capable of combined and tumor-targeted delivery of therapeutic and diagnostic agents can greatly enhance the efficacy of cancer therapy and the accuracy of diagnosis/prognosis, which can pave the road for personalized medicine.[1−10] As a diagnostic technique, magnetic resonance imaging (MRI) is one of the most powerful, non-invasive imaging modalities used in clinical medicine today; however, higher MRI sensitivity is needed to accurately diagnose/prognose early stage cancers. One way to enhance MRI sensitivity is to use superparamagnetic iron oxide (SPIO) nanoparticles (NPs) as MRI contrast agents.[11,12] Hence, combined delivery of an anticancer drug and SPIO NPs to tumor sites can improve the therapeutic efficacy, reduce undesirable side effects, and provide enhanced MRI tumor contrast, which may allow physicians to predict the therapeutic efficiency of the treatment based on the biodistribution of the nanomedicine and also non-invasively monitor cancer progression.[13−18]

There are many factors that can affect the performance of multifunctional nanocarriers for targeted cancer therapy and diagnosis/prognosis, including their *in vivo* stability, tumor-targeting ability, drug/agent loading levels, and drug release profile.[19,20] Here, we report the development of multifunctional SPIO/doxorubicin (DOX)-loaded polymer vesicles formed by heterofunctional amphiphilic triblock copolymers that provided pH-controlled drug release, excellent *in vivo* stability, high DOX and SPIO loading levels, both passive and active tumor-targeting abilities, and significantly enhanced MRI contrast (Scheme 1).

Similar to liposomes, polymer vesicles can simultaneously deliver hydrophilic and hydrophobic agents encapsulated in their

*Address correspondence to sgong@engr.wisc.edu.

Received for review July 16, 2010 and accepted October 12, 2010.

Published online October 19, 2010. 10.1021/nn101670k

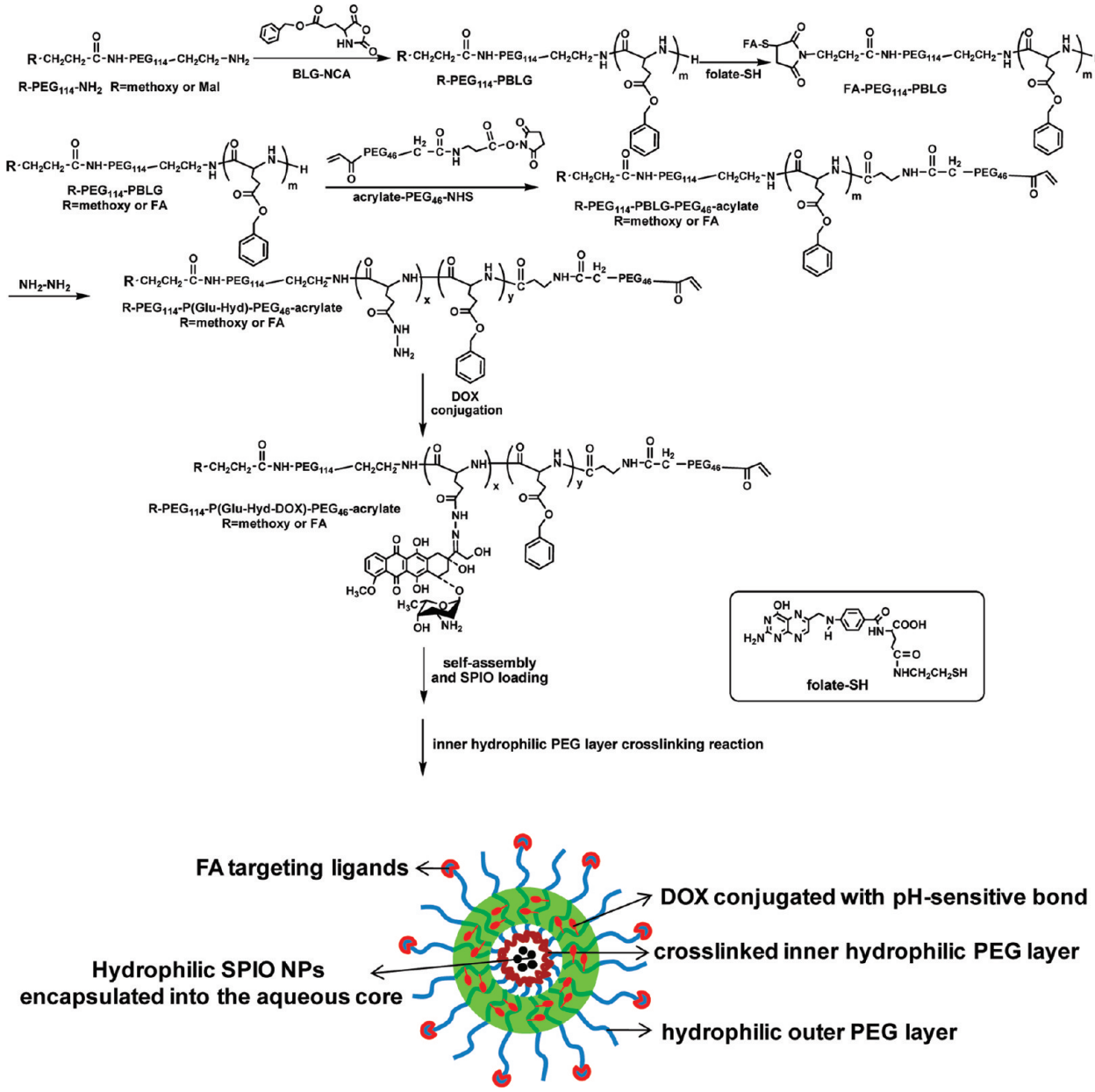

Scheme 1. Synthetic scheme of the amphiphilic triblock copolymers and the preparation process of the SPIO/DOX-loaded vesicles with cross-linked inner hydrophilic PEG layers.

aqueous core and hydrophobic membrane, respectively. However, compared with liposomes, polymer vesicles offer many more possibilities to control their physical, chemical, and biological properties by tailoring the block lengths, block chemistry, and functionality.[21] Thus, polymer vesicles can exhibit many unique properties that may not be achieved by other types of nanocarriers, making them extremely attractive for multifunctional nanomedicine.[22] Most polymer vesicles reported thus far are formed by amphiphilic diblock copolymers.[23−25] We chose to use heterofunctional amphiphilic triblock copolymers, such as R(R = folate (FA) or methoxy)-poly(ethylene glycol)(M_w:5000)-poly(glutamate hydrozone doxorubicin)-poly(ethylene glycol)(M_w:2000)-acrylate (*i.e.*, R(R = FA or methoxy)-PEG_{114}-P(Glu-Hyd-DOX)-PEG_{46}-acrylate), for this study due to the following considerations. Many of the most widely studied drug nanocarriers, including polymer micelles and vesicles as well as liposomes, are formed by self-assembly, which is a dynamic process. Thus, the *in vivo* stability of such self-assembled nanocarriers is affected by many factors including polymer concentration, shear force, temperature, pressure, and interaction with blood components.[26,27] If the nanocarriers disassemble in the bloodstream, it can lead to a premature burst-release of high concentrations of drug and MRI contrast agent, thereby leading to poor targeting, reduced therapeutic effect, and potential serious toxicity. Hence, there is a significant need to stabilize the self-assembled nanocarriers, which can be achieved by se-

lectively cross-linking the nanocarriers. The two PEG segments of the triblock copolymers that we designed and synthesized had different molecular weights (5000 *vs* 2000 Da). Due to thermodynamic stabilization, the long PEG segments bearing FA or methoxy groups were mostly segregated to the outer hydrophilic PEG layer of the vesicle, thereby providing active tumor-targeting abilities; while the short PEG segments bearing the acrylate groups were mostly segregated to the inner hydrophilic PEG layer of the vesicle, thereby making it possible to cross-link the vesicle *via* free radical polymerization for enhanced *in vivo* stability. Another advantage of using triblock copolymers *versus* diblock copolymers in this case is that stable vesicles can be achieved by only cross-linking the inner hydrophilic PEG layer. For vesicles formed by diblock copolymers, both the inner and outer hydrophilic PEG layers have to be cross-linked in order to achieve excellent *in vivo* stability. However, cross-linking both PEG layers can significantly reduce the drug release rate. In our design, the anticancer drug, DOX, was conjugated onto the hydrophobic polyglutamate segment *via* a pH-sensitive hydrazone linkage, thereby resulting in a pH-triggered DOX release profile. Since the DOX molecules were outside of the cross-linked inner PEG layer, the drug release rate would not be significantly affected by the cross-linked inner PEG layer. A pH-responsive drug release profile would ensure minimal drug loss during circulation in the bloodstream but relatively rapid drug release once internalized by the tumor cells. Higher DOX loading levels can also be achieved *via* covalent DOX conjugation. A cluster of hydrophilic SPIO NPs was encapsulated into the aqueous cores of the stable vesicles to provide ultrasensitive MRI detection. In addition, PEGylated vesicles with controlled particle sizes are expected to significantly increase their *in vivo* circulation time by avoiding renal excretion and decreasing uptake by the reticuloendothelial system (RES). This increased circulation time in the bloodstream would allow for both increased passive targeting of the vesicles through the enhanced permeability and retention (EPR) effect and increased active targeting *via* the folate receptor. Finally, multifunctional SPIO/drug-loaded polymer vesicles formed by triblock copolymers that exhibit pH-controlled drug release, excellent *in vivo* stability, active tumor-targeting, and significantly enhanced MRI contrast have not been reported previously.

RESULTS AND DISCUSSION

Synthesis of Heterofunctional Triblock Copolymers. To form the multifunctional polymer vesicles, heterofunctional amphiphilic triblock copolymers, R (R = folate (FA) or methoxy)-poly(ethylene glycol) (long chain, M_w:5000)-poly(glutamate hydrazone doxorubicin)-poly(ethylene glycol) (short chain, M_w:2000)-acrylate (*i.e.*, R(FA or methoxy)-PEG_{114}-P(Glu-Hyd-DOX)-PEG_{46}-acrylate)) were rationally designed and successfully synthesized (Scheme 1). First, the maleimide-PEG_{114}-poly(γ-benzyl-L-glutamate) (Mal-PEG_{114}-PBLG) copolymers were synthesized *via* ring-opening polymerization of γ-benzyl-L-glutamate-*N*-carboxyanhydride (BLG-NCA) using Mal-PEG_{114}-NH_2 as a macromolecular initiator.[25] To fabricate the polymer vesicles, three copolymers with different PBLG molecular weights, while using the same PEG segment (*i.e.*, 114 repeat units, M_w 5000), were prepared by controlling the feed ratio and reaction time. The number of BLG repeat units in the PBLG segment of the three Mal-PEG_{114}-PBLG copolymers synthesized was 119, 171, and 210, according to the ^{1}H NMR analysis (Figure S1). The FA-PEG_{114}-PBLG copolymer was synthesized *via* a reaction between the Mal-PEG_{114}-PBLG copolymer and the thiol-functionalized folate (*i.e.*, FA-SH), which was prepared through a reaction between the γ-carboxy group of FA and the amino group of 2-aminoethanethiol in the presence of *N*,*N*′-dicyclohexylcarbodiimide (DCC) and *N*-hydroxysuccinimide (NHS). ^{1}H NMR analysis confirmed that FA was successfully conjugated onto the PEG because the characteristic NMR peak of the maleimide group disappeared after the reaction (Figure S2). Subsequently, the FA-PEG_{114}-PBLG-acrylate copolymer was obtained through a reaction between the NHS group of NHS-PEG-acrylate (M_w of PEG 2000; 46 repeat units) and the terminal NH_2 group of the FA-PEG_{114}-PBLG copolymer. Among the three types of triblock copolymers synthesized (*i.e.*, PBLG with 119, 171, and 210 BLG repeat units), the FA-PEG_{114}-PBLG-acrylate copolymer with 171 BLG repeat units demonstrated the best ability to self-assemble into stable vesicles under the same experimental conditions (Figure S3). For the copolymer with 119 repeat units, the vesicles formed were very irregular; for the copolymer with 210 repeat units, they assembled into vesicles having a thick membrane and were not stable in aqueous solution. Specifically, precipitates were found upon storage at 4 °C for three days. The different morphologies self-assembled by these three different triblock copolymers may be due to the different hydrophobic/hydrophilic ratios of the triblock copolymers. Thus, the triblock copolymer FA-PEG_{114}-$PBLG_{171}$-PEG_{46}-acrylate was chosen for subsequent studies (Figure 1, Top).

In order to conjugate the anticancer drug DOX to the triblock copolymer, the benzyl groups of the FA-PEG_{114}-$PBLG_{171}$-PEG_{46}-acrylate were substituted with hydrazide groups for DOX binding by an ester-amide exchange (EAE) aminolysis reaction.[28] The degree of benzyl substitution was optimized by controlling the reaction time to ensure ease of polymer vesicle formation. The number of hydrazide groups conjugated onto the PBLG segments was calculated by comparing the integrals of the proton signals f (corresponding to the $-CH_2-$ groups of PBLG segments, which can be cleaved *via* the aminolysis reaction) before and after the aminolysis reaction through hydrazine and was con-

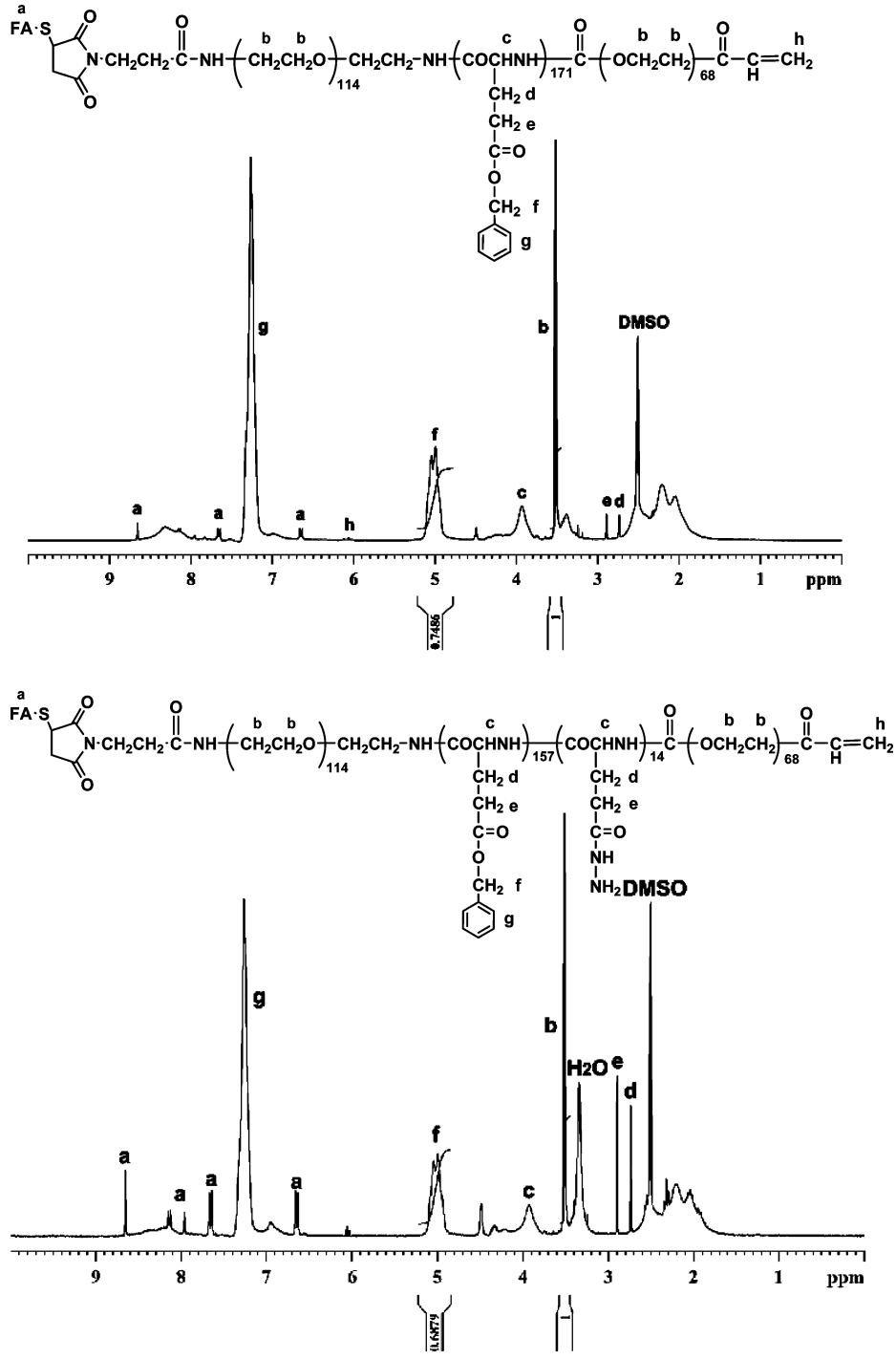

Figure 1. ^{1}H NMR spectra of the FA-PEG$_{114}$-PBLG$_{171}$-PEG$_{46}$-acrylate (Top) and FA-PEG$_{114}$-PBLG$_{157}$-Hyd$_{14}$-PEG$_{46}$-acrylate (Bottom) triblock copolymers.

sidered to be equal to the number of missing BLG repeat units of the copolymers after the aminolysis reaction. For instance, it was found that the triblock copolymer FA-PEG$_{114}$-PBLG$_{157}$-Hyd$_{14}$-PEG$_{46}$-acrylate with 14 hydrazide groups could easily self-assemble into polymer vesicles after DOX conjugation (Figure 1, Bottom). DOX was conjugated onto the triblock copolymers through an acid-sensitive hydrazone bond. The DOX loading content in the copolymers was measured by first cleaving the hydrazone linkers in 0.1 N HCl solution. Subsequently, the amount of DOX released was determined to be 14 wt % *via* UV spectroscopy based on the absorbance intensity at 485 nm using a DOX calibration curve generated in 0.1 N HCl solution. On the basis of the DOX loading level (14 wt %), it was estimated that 13 out of the 14 hydrazide groups per FA-PEG$_{114}$-PBLG$_{157}$-Hyd$_{14}$-PEG$_{46}$-acrylate copolymer chain were conjugated with DOX molecules. To control the molar ratio of the FA targeting ligand in the self-assembled vesicles, FA-free triblock copolymer (*i.e.*,

methoxy-PEG_{114}-$PBLG_{157}$-Hyd_{14}-DOX_{13}-PEG_{46}-acrylate) was synthesized following the same approach using methoxy-PEG_{114}-NH_2 as a macromolecular initiator as discussed above.

Polymer Vesicle Formation. Stable polymer vesicles were formed by mixing a certain amount (6 wt %) of the triblock copolymer mixture (*i.e.*, FA-conjugated FA-PEG_{114}-P(Glu-Hyd-DOX)-PEG_{46}-acrylate and FA-free methoxy-PEG_{114}-P(Glu-Hyd-DOX)-PEG_{46}-acrylate) at a specific molar ratio with deionized (DI) water directly under stirring without the use of any cosolvent followed by ultrasonication at room temperature for 30 min. The FA-free triblock copolymer was used to control the molar ratio of the FA targeting ligand in the polymer vesicles. It is known that folate moieties with pterin heterocycles can self-assemble in an aqueous solution by hydrogen bonding and stacking interactions.[29] As a result, nanocarriers with a high FA molar ratio exhibit poor stability in aqueous solution.[30] In addition, the possible formation of dimers, trimers, or self-assembled tubular quarters[29] at higher FA concentrations is very unfavorable for tumor cell targeting because the folate receptor can only bind to one FA molecule; thus, the self-assembled FA multimers are incapable of binding to the folate receptors. In this study, the FA targeting ligand was controlled to 3% in the mixture. As discussed later, we hypothesized that, due to thermodynamic stabilization, the long hydrophilic PEG segments bearing FA molecules were mostly segregated into the outer hydrophilic PEG layers of the vesicles, while the short hydrophilic segments bearing the acrylate groups were mostly segregated into the inner hydrophilic PEG layers.[31] Figure 2a shows a TEM image of the polymer vesicles self-assembled using a mixture of the FA-conjugated and FA-free triblock copolymers with 3% FA targeting ligand. Polymer vesicles with an average diameter of approximately 140 nm were successfully formed in DI water. The thickness of the hydrophobic membrane was approximately 30 nm. Compared to liposomes, vesicles formed using triblock copolymers and having a much thicker membrane are more durable/robust and offer numerous possibilities to tune the physiochemical and biological properties needed for nanomedicine.[32] For instance, in this study, the anticancer drug DOX was conjugated to the hydrophobic polyglutamate segments which formed the hydrophobic membrane *via* a pH-sensitive linker.

To obtain excellent *in vivo* stability, the inner hydrophilic PEG layers of the vesicles were cross-linked through the terminal acrylate groups attached to the short PEG segments *via* free radical polymerization in a water solution following a previously reported method with a slight modification.[33] The water-soluble initiator $K_2S_2O_8$ was loaded into the aqueous cores of the polymer vesicles dissolved in DI water, and the solution was allowed to react at 45 °C for 3 h. The cross-linking reaction was confirmed by ^{1}H NMR spectroscopy. Similar

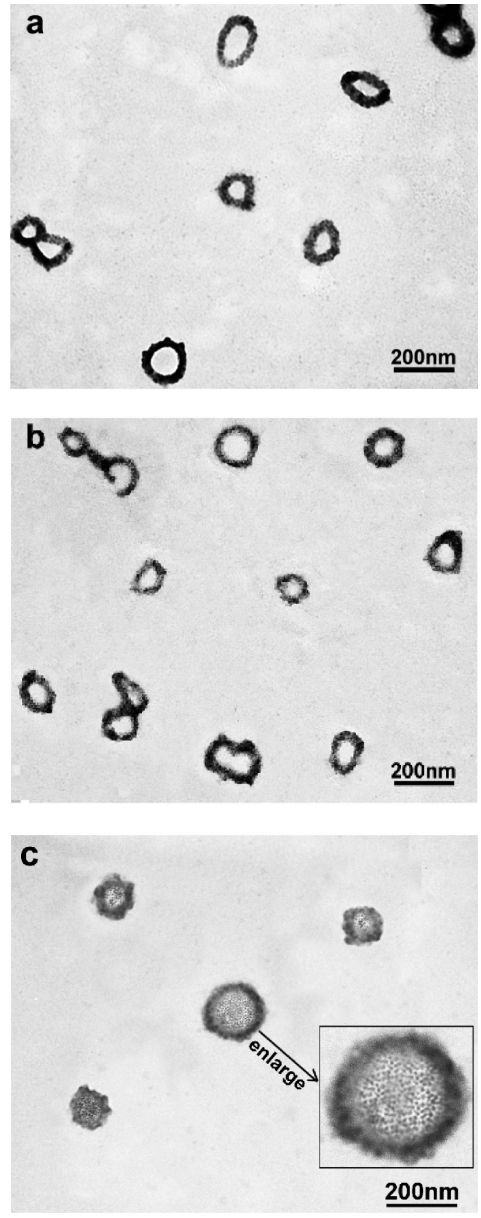

Figure 2. TEM images of various types of polymer vesicles formed by R (methoxy or FA)-PEG_{114}-P(Glu-Hyd-DOX)-PEG_{46}-acrylate triblock copolymers. (a) DOX-loaded polymer vesicles with non-cross-linked inner hydrophilic PEG layers; (b) DOX-loaded polymer vesicles with cross-linked inner hydrophilic PEG layers; and (c) SPIO/DOX-loaded polymer vesicles with cross-linked inner hydrophilic PEG layers.

to liposomes, the hydrophobic membrane of the polymer vesicles formed by amphiphilic AB diblock copolymers is an interdigitated bilayer. In contrast, the hydrophobic membrane of the polymer vesicles formed by the amphiphilic ABA triblock copolymers used in this study is a single layer formed by the hydrophobic B polymer segment. Thus, polymer vesicles formed by such triblock copolymers can be stabilized by only cross-linking the inner hydrophilic PEG layers. Since the anticancer drug was conjugated to the hydrophobic polyglutamate segments outside of the inner hydrophilic PEG layer, the DOX release rate would not be sig-

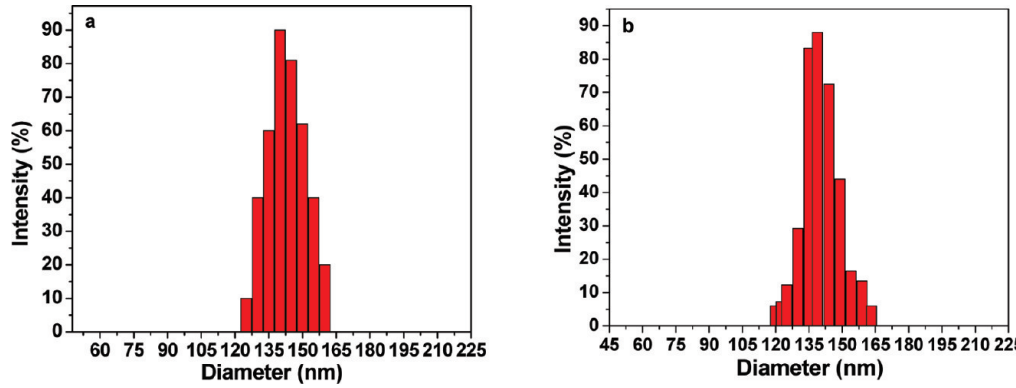

Figure 3. DLS analysis of the SPIO/DOX-loaded vesicles with non-cross-linked inner hydrophilic PEG layers (a) and SPIO/DOX-loaded vesicles with cross-linked inner hydrophilic PEG layers (b) formed by R (R = methoxy or FA)-PEG$_{114}$-P(Glu-Hyd-DOX)-PEG$_{46}$-acrylate triblock copolymers.

nificantly affected. Figure 2b shows a TEM image of the polymer vesicles with cross-linked inner hydrophilic PEG layers. As shown in Figure 2a,b, the size and morphology of the polymer vesicles did not change after the cross-linking reaction. This observation supports our hypothesis that the short hydrophilic PEG segments were mostly segregated into the inner hydrophilic PEG layer; otherwise, vesicle aggregation caused by inter-vesicle cross-linking may be observed. Figure 2c shows a TEM image of the SPIO/DOX-loaded polymer vesicles with cross-linked inner hydrophilic PEG layers. As shown in Figure 2c, the SPIO NPs were uniformly dispersed in the aqueous cores of the polymer vesicles, forming a cluster of SPIO NPs which can significantly enhance the T_2 relaxivity. Up to 46 wt % SPIO NPs can be loaded into these vesicles, which could potentially allow the detection of the SPIO/DOX-loaded vesicles at nanomolar concentrations.[34] The size and size distribution of the SPIO/DOX-loaded vesicles were further analyzed by dynamic light scattering (DLS). The mean hydrodynamic diameter of the SPIO/DOX-loaded vesicles with non-cross-linked inner hydrophilic PEG layers was 146 $\pm$ 2 nm (Figure 3a, polydispersity index (PDI) = 0.207 $\pm$ 0.004), while the mean hydrodynamic diameter of the SPIO/DOX-loaded vesicles with cross-linked inner hydrophilic PEG layers was 152 $\pm$ 4 nm (Figure 3b, PDI = 0.231 $\pm$ 0.002). The DLS results were consistent with the TEM finding in that the cross-linking reaction did not affect the size or size distribution of the SPIO/DOX-loaded polymer vesicles. To determine the potential *in vivo* stability of the vesicles, the stability of FA-conjugated SPIO/DOX-loaded vesicles in PBS containing 15% human serum was evaluated by DLS analysis. As shown in Figure S4, the size and size distribution of the vesicles did not change appreciably following incubation in serum for 3 days. It should also be noted that the vesicle solution did not show any aggregate formation upon storage for one week at 4 °C.

Investigation of the Self-Assembly Behavior of the Heterofunctional Amphiphilic Triblock Copolymers. The self-assembly behavior of the heterofunctional amphiphilic triblock copolymers having two different PEG segments was further investigated in order to demonstrate the preferential segregation of the short and long PEG segments of the triblock copolymers in the resulting polymer vesicles. To do so, rhodamine B, a fluorescent probe, was conjugated onto the terminal end of the short hydrophilic PEG segment of the triblock copolymer (*i.e.*, Mal-PEG$_{114}$-PBLG$_{171}$-PEG$_{46}$-rhodamine B) *via* a reaction between the carboxy group of rhodamine B and the hydroxyl group of PEG in the presence of DCC and 4-dimethylaminopyridine (DMAP). The self-assembly behavior of the Mal-PEG$_{114}$-PBLG$_{171}$-PEG$_{46}$-rhodamine B triblock copolymer in aqueous solution was studied in real-time using fluorescence spectroscopy. As shown in Figure 4, the fluorescence intensity of rhodamine B did not change markedly during the initial periods of the mixing process (*e.g.*, after 10 or 60 min stirring). However, after 5 h stirring followed by 30 min sonication, the fluorescence intensity of rhodamine B decreased significantly, which can be attributed to the formation of vesicles facilitated by ultrasonic sonication. In addition, it was observed that the fluorescence intensity of rhodamine B no longer changed after stable vesicles were formed. The significant reduction of fluorescence intensity associated with vesicle formation

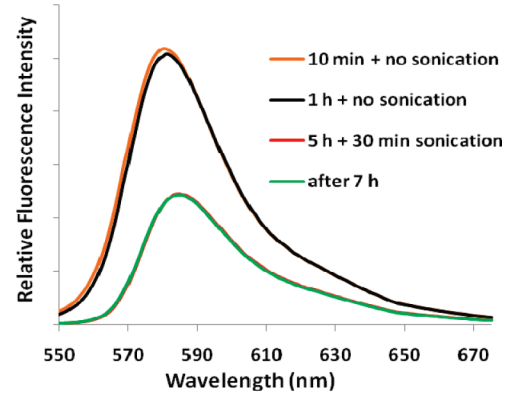

Figure 4. Change in the fluorescence intensity of rhodamine B during the various stages of the polymer vesicle formation process based on the Mal-PEG$_{114}$-PBLG-PEG$_{46}$-rhodamine B triblock copolymer.

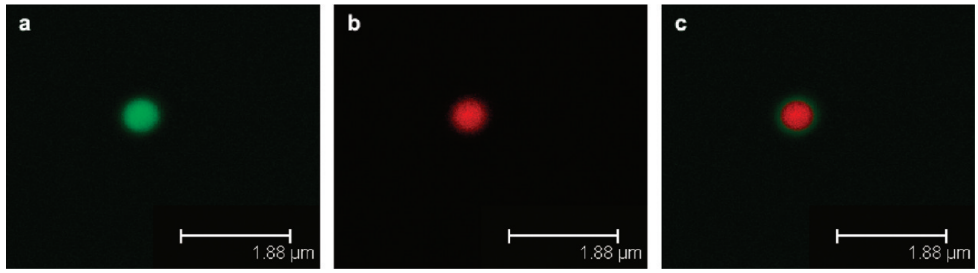

Figure 5. CLSM images of the $DiOC_{18}$ (fluorescence probe)-loaded polymer vesicles formed by Mal-PEG_{114}-PBLG-PEG_{46}-DOX triblock copolymer using the same excitation but different emission wavelengths (a) λ_{ex} = 485 nm, λ_{em} = 501 nm for $DiOC_{18}$; (b) λ_{ex} = 485 nm, λ_{em} = 595 nm for DOX; and (c) physically overlaid image of panels a and b.

may be partially attributed to rhodamine B self-quenching resulting from the preferential segregation of the short PEG segments bearing rhodamine B in the aqueous vesicle cores. Moreover, confocal laser scanning microscopy (CLSM) analysis was used to further investigate the vesicle formation behavior of the Mal-PEG_{114}-$PBLG_{171}$-PEG_{46}-DOX triblock copolymer. DOX, the self-fluorescent model anticancer drug, was conjugated onto the short PEG segments of the Mal-PEG_{114}-$PBLG_{171}$-PEG_{46} triblock copolymers (*i.e.*, Mal-PEG_{114}-$PBLG_{171}$-PEG_{46}-DOX) *via* a carbamate linkage. To form the carbamate linkage between the primary amine group of DOX and the triblock copolymer, the terminal hydroxyl group of the Mal-PEG_{114}-$PBLG_{171}$-PEG_{46} triblock copolymer was first activated with *p*-nitrophenyl chloroformate in a chloroform solution in the presence of pyridine at room temperature. The vesicles were prepared by mixing the Mal-PEG_{114}-$PBLG_{171}$-PEG_{46}-DOX triblock copolymer directly with the water/THF (10:1) mixture solution that contained a hydrophobic green fluorescent probe ($DiOC_{18}$) under sonication. To allow CLSM analysis of the vesicle structure, larger diameter vesicles (500−600 nm) were prepared by adjusting the power level and time of sonication. The hydrophobic $DiOC_{18}$ was expected to be encapsulated into the hydrophobic membrane of the polymer vesicle. Figure 5 shows a series of CLSM images of the same fluorescence-labeled vesicle. Figure 5a shows the vesicle as a green fluorescent sphere, indicating that $DiOC_{18}$ was successfully loaded into the membrane of the vesicle, while Figure 5b shows red fluorescence in the same vesicle, indicating the presence of DOX molecules. Figure 5c shows the physically overlaid images of the green (Figure 5a) and red (Figure 5b) fluorescence. The diameter of the sphere generated from the green fluorescence was visibly larger than that from the red fluorescence, suggesting that $DiOC_{18}$ was encapsulated in the hydrophobic membrane while DOX conjugated onto the short PEG segments was localized within the inner core of the vesicle. Lastly, as discussed previously, the size and morphology of the polymer vesicles did not change after the cross-linking reaction (Figures 2a,b). Collectively, these results support our hypothesis on the preferential segregation of the short and long PEG segments of the triblock copolymers in the polymer vesicles. Namely, the short hydrophilic PEG segments were mostly segregated into the inner hydrophilic PEG layers, while the long hydrophilic PEG segments were mostly segregated into the outer hydrophilic PEG layers. The preferential segregation of the PEG segments with different molecular weights may be due to the repulsion among the outer-layer long PEG chains being stronger than that of the inner-layer short PEG chains; thus, the curvature is maintained in a thermodynamically stable manner.[31] Preferential segregation of such heterofunctional amphiphilic block copolymers provides a convenient way to fabricate NPs with multifunctionalities.

Evaluation of pH-Controlled Drug Release Profiles. The DOX release profiles of the SPIO/DOX-loaded vesicles with either cross-linked or non-cross-linked inner hydrophilic PEG layers was studied at pH 5.3 and 7.4. The UV absorption spectra of DOX at different pH values (5.3, 7.4, and 0.1 N HCl) were collected using UV spectrophotometry, and it was found that changes in pH value had no apparent effect on the UV absorption of DOX (Figure S5). As shown in Figure 6, at pH 7.4, a negligible amount of DOX release was observed from both types of vesicles (cross-linked or non-cross-linked). This is a desirable characteristic because, during circulation in the bloodstream, where the pH value is ~7.4, DOX conju-

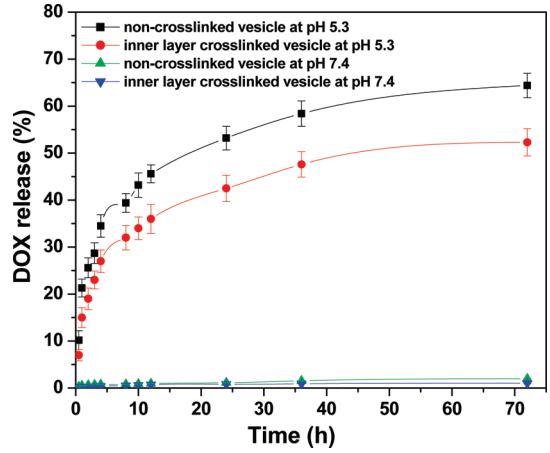

Figure 6. *In vitro* DOX release profiles of the SPIO/DOX-loaded polymer vesicles with either cross-linked or non-cross-linked inner hydrophilic PEG layers at two different pH values (*i.e.*, pH 5.3 and 7.4). Each data point was measured in triplicate.

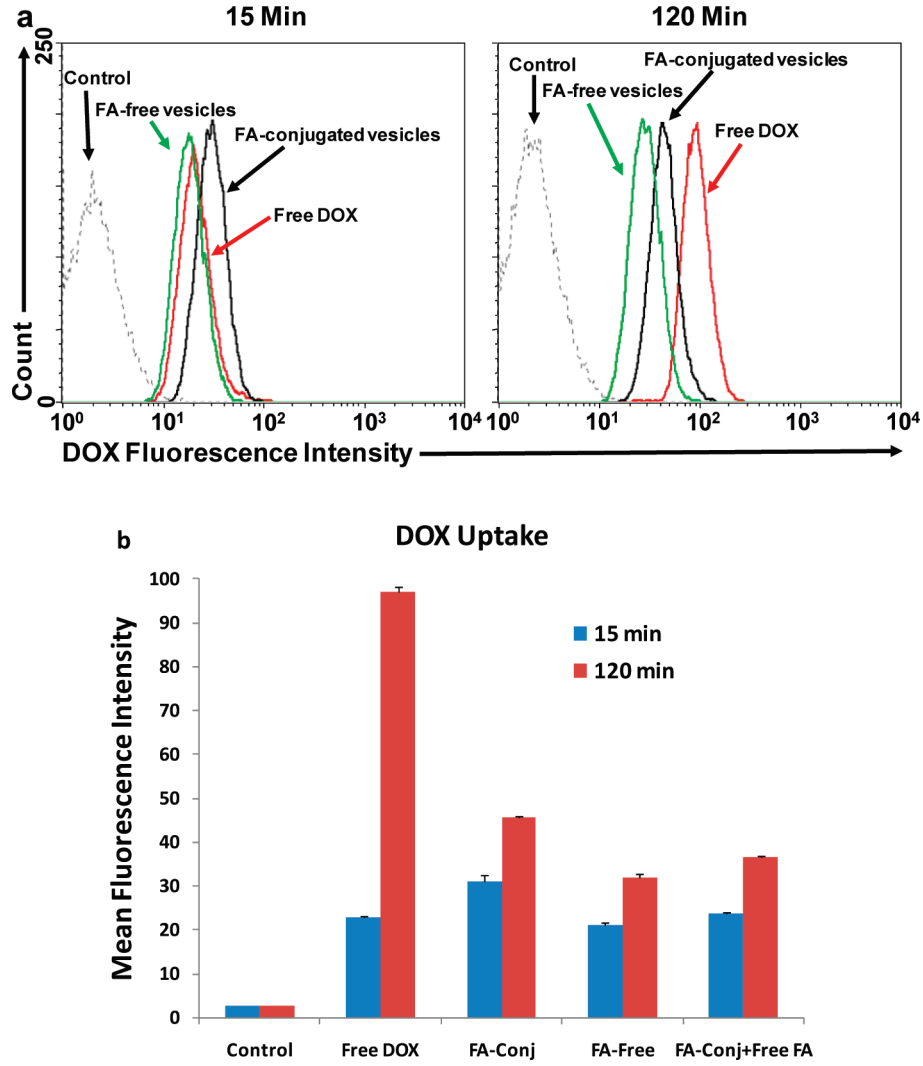

Figure 7. (a) DOX fluorescence intensity of HeLa cells incubated with free DOX, FA-conjugated, and FA-free SPIO/DOX-loaded vesicles with cross-linked inner hydrophilic PEG layers at 37 °C for 15 and 120 min (DOX concentration = 20 μg/mL) measured by flow cytometry. (b) DOX mean fluorescence intensity (MFI) of the HeLa cells incubated with free DOX, FA-conjugated, and FA-free SPIO/DOX-loaded vesicles with cross-linked inner hydrophilic PEG layers for 15 and 120 min (untreated cells were used as control; each treatment group and time point were done in triplicate).

gated onto the drug nanocarriers would not be released prematurely into the bloodstream before reaching the targeted tumor sites. At pH 5.3, a two-stage release profile was observed; namely, an initial rapid release stage occurred during the first 10 h followed by a more sustained release stage. As discussed previously, this pH-dependent DOX release behavior is highly desirable for targeted cancer therapy because it can significantly minimize the amount of premature drug release during circulation in the bloodstream yet provide a sufficient amount of drug to effectively kill the cancer cells once the nanocarriers are internalized and enter the endocytic pathway. Moreover, at pH 5.3, the DOX release rate of the SPIO/DOX-loaded vesicles with non-cross-linked inner hydrophilic PEG layers was faster than that of the vesicles with cross-linked inner hydrophilic PEG layers within the first 10 h. Cross-linking can effectively preserve the structural integrity of polymer vesicles,[35,36] which may lead to a slower drug release rate.[33]

Cell Uptake and Biodistribution Studies. To study the effects of FA targeting ligand on the cellular uptake and biodistribution of the SPIO/DOX-loaded vesicles with cross-linked inner hydrophilic PEG layers, both flow cytometry and CLSM analysis were conducted using HeLa tumor cells (derived from human cervical cancer). Figure 7a shows the DOX fluorescence intensity of HeLa cells incubated with free DOX and FA-conjugated and FA-free SPIO/DOX-loaded vesicles with cross-linked inner hydrophilic PEG layers for 15 and 120 min, respectively, measured by flow cytometry. The flow cytometry analysis clearly demonstrated that FA targeting ligand effectively enhanced the cellular uptake of the SPIO/DOX-loaded vesicles at both time points, presumably facilitated by the folate receptor-mediated endocytosis process. In addition, the higher cellular uptake of free

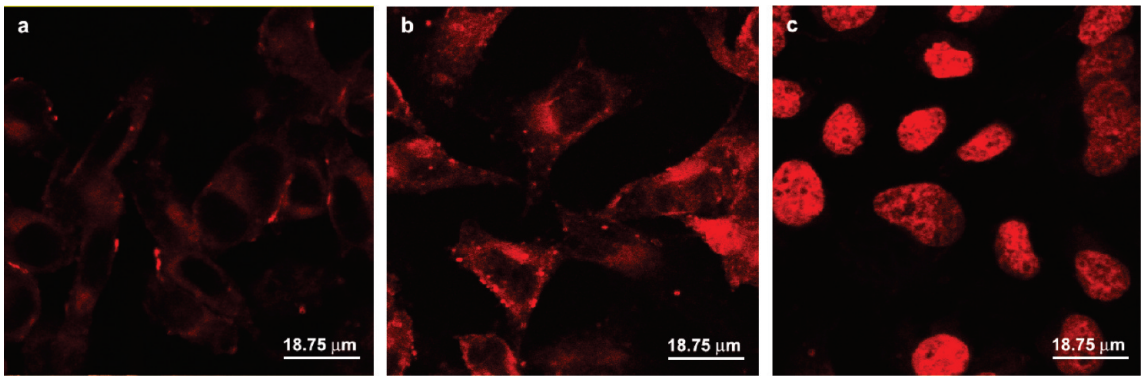

Figure 8. CLSM images of HeLa cells incubated with (a) FA-free or (b) FA-conjugated SPIO/DOX-loaded vesicles with cross-linked inner hydrophilic PEG layers, or (c) free DOX at 37 °C for 120 min (DOX concentration = 20 μg/mL).

DOX compared with SPIO/DOX-loaded polymer vesicles after 2 h incubation can be attributed to the different cellular uptake mechanisms. Free DOX is known to be transported into cells *via* diffusion,[37] while SPIO/DOX-loaded vesicles are taken up by the HeLa cells *via* an endocytosis process.[38] Figure 7b shows the DOX mean fluorescence intensity (MFI) of the HeLa cells after being incubated with free DOX and FA-conjugated and FA-free SPIO/DOX-loaded vesicles with cross-linked inner hydrophilic PEG layers (equivalent DOX concentration = 20 μg/mL) for 15 and 120 min, respectively. The MFI of HeLa cells incubated with FA-conjugated vesicles was approximately 1.5-fold higher than that of cells incubated with FA-free vesicles. Moreover, FA blocking experiments demonstrated that the cellular uptake level of FA-conjugated vesicles in the presence of free FA (present in the cell culture medium) was reduced and became essentially equivalent to that of FA-free vesicles. This observation further supports the concept that the cell uptake of FA-conjugated vesicles was facilitated by the folate receptor-mediated endocytosis process.

CLSM was used to further characterize and compare the cell uptake and intracellular distribution of free DOX and FA-conjugated and FA-free SPIO/DOX-loaded vesicles with cross-linked inner hydrophilic PEG layers in HeLa cells after 2 h of incubation. As shown in Figure 8, the DOX fluorescence intensity of HeLa cells incubated with FA-conjugated SPIO/DOX-loaded vesicles was significantly higher than that of cells incubated with FA-free vesicles, which was consistent with the flow cytometry results. In addition, while free DOX was primarily localized in the nuclei of the HeLa cells, DOX delivered *via* the SPIO/DOX-loaded vesicles was largely accumulated in the cytosol of the Hela cells after 2 h of incubation, which again can be attributed to the different cellular uptake mechanisms between free DOX (*i.e.*, diffusion through the cell membrane) and the SPIO/DOX-loaded vesicles (*i.e.*, endocytosis). Eventually, DOX released from the SPIO/DOX-loaded vesicles would also diffuse from the cytosol into the nuclei of the HeLa cells, where it can interrupt DNA replication and eventually lead to cell death.[39]

Cytotoxicity Study. The cytotoxicity of free DOX and FA-conjugated and FA-free SPIO/DOX-loaded vesicles with cross-linked inner hydrophilic PEG layers against HeLa cells was evaluated using an MTT (3-(4,5-dimethylthiazol-2-yl)-2,5-diphenyltetrazolium bromide) assay. HeLa cells were treated with free DOX and FA-conjugated and FA-free SPIO/DOX-loaded vesicles at various DOX concentrations. As shown in Figure 9, the viability of HeLa cells depended on the DOX concentration; however, a much stronger dependence was observed for HeLa cells incubated with the SPIO/DOX-loaded vesicles compared with free DOX. In addition, the cytotoxicity of FA-conjugated SPIO/DOX-loaded vesicles was consistently higher than that of FA-free vesicles at all DOX concentrations tested due to the enhanced cellular uptake attributed to folate receptor-mediated endocytosis. Moreover, at the same DOX concentration, free DOX showed higher cytotoxicity than the SPIO/DOX-loaded vesicles due to the different cellular uptake and drug release behavior between free DOX and SPIO/DOX-loaded vesicles. DOX is a DNA intercalator. As indicated by the CLSM analysis, once inside the cell free, DOX can rapidly diffuse into the cell nuclei and effectively inhibit DNA replication in the cancer cells. By contrast, DOX conjugated onto the SPIO/DOX-loaded vesicles was released in a more controlled manner initially in the acidic endocytic compartments followed by diffusion into the cytosol and finally into the cell nuclei.

Relaxivity Measurement. In general, the effect of an MRI contrast agent is assessed based on its longitudinal and transverse relaxivities, r_1 and r_2, which reflect the ability of the contrast agent to alter T_1 (spin−lattice relaxation) and T_2 (spin−spin relaxation), respectively. Relaxivities can be calculated through the linear least-squares fitting of 1/relaxation time (s^{-1}) *versus* the iron concentration (mM Fe). The relaxation times were measured at 4.7 T on a Varian Inova MRI scanner at room temperature. SPIO NPs are generally used as a T_2 contrast agent. Figure 10a shows the measurement of

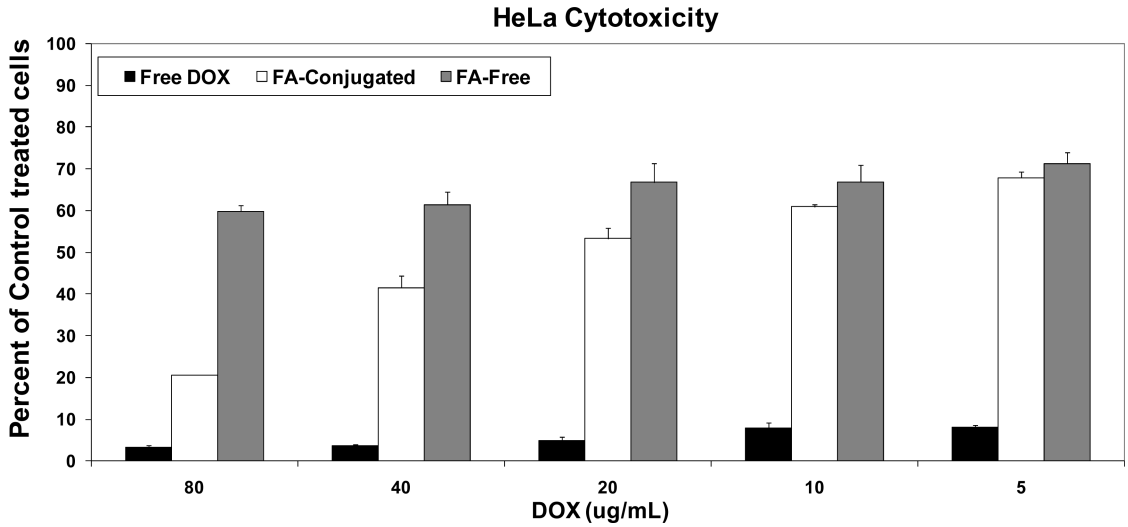

Figure 9. Cytotoxicity of free DOX and FA-free and FA-conjugated SPIO/DOX-loaded vesicles with cross-linked inner hydrophilic PEG layers against HeLa cells at different DOX concentrations (incubation time = 48 h; each treatment group was done in triplicate).

the r_2 relaxivities for Feridex, a commercially available SPIO-based MRI contrast agent, and the FA-conjugated SPIO/DOX-loaded vesicles with cross-linked inner hydrophilic PEG layers. The r_2 of Feridex was 111.5 Fe mM^{-1} s^{-1}, which was very close to the reported value (105 Fe mM^{-1} s^{-1}) measured at 4.7 T,[40] while the r_2 of the SPIO/DOX-loaded vesicles was 346.1 Fe mM^{-1} s^{-1}, representing an approximate 3.2-fold enhancement. The short distance between the clustered SPIO NPs inside the vesicle's core may permit magnetic coupling between the NPs, leading to a synergistic increase in r_2.[12,41−44] To further evaluate the detection sensitivity of the SPIO/DOX-loaded vesicles, T_2-weighted images were also collected at 4.7 T (spin−echo sequence, TR = 8000 ms, TE = 12.75 ms, room temperature). Figure 10b shows the T_2-weighted images of the SPIO/DOX-loaded vesicles and Feridex at various Fe concentrations. For a given Fe concentration, the SPIO/DOX-loaded vesicle solutions showed a much darker image compared to Feridex; thus, the SPIO/DOX-loaded vesicles can serve as a highly efficient T_2 contrast agent.

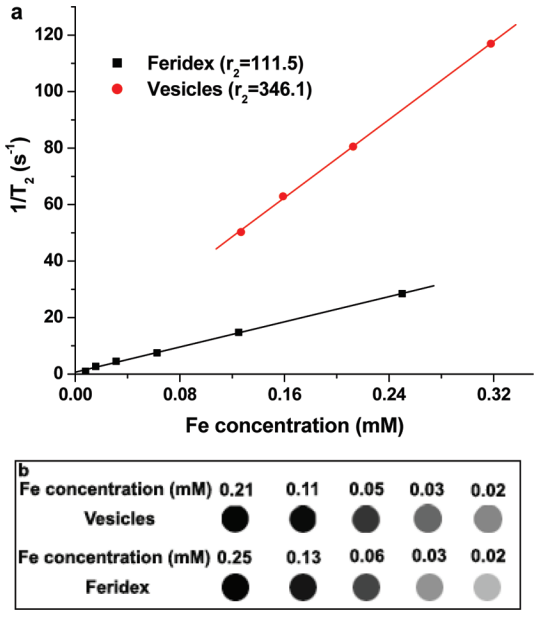

Figure 10. (a) T_2 relaxation rates ($1/T_2$, s^{-1}) as a function of iron concentration (mM) for both FA-conjugated SPIO/DOX-loaded vesicles and Feridex. (b) T_2-weighted MRI images of the FA-conjugated SPIO/DOX-loaded vesicles and Feridex.

CONCLUSIONS

Multifunctional stable and pH-responsive SPIO/DOX-loaded polymer vesicles for combined and tumor-targeted drug delivery and ultrasensitive MR imaging have been developed. These multifunctional polymer vesicles were formed in an aqueous solution by self-assembly of heterofunctional amphiphilic triblock copolymers with two different PEG segments, R(R = FA or methoxy)-PEG_{114}-P(Glu-Hyd-DOX)-PEG_{46}-acrylate. Due to thermodynamic stabilization, the long hydrophilic PEG segments bearing the FA targeting ligand were mostly segregated into the outer hydrophilic PEG layers of the vesicles, thereby providing the vesicles with active tumor-targeting ability, while the short hydrophilic PEG segments bearing the acrylate groups were mostly segregated to the inner hydrophilic PEG layers, thereby making it possible to cross-link the inner PEG layers *via* free radical polymerization for enhanced *in vivo* stability. The anticancer drug (DOX) was conjugated onto the hydrophobic polyglutamate polymer segments that formed the hydrophobic membrane of the vesicles through an acid-cleavable hydrazone bond to achieve pH-controlled release, while the SPIO NPs were encapsulated into the aqueous cores of the vesicles for enhanced MRI contrast. These multifunctional SPIO/DOX-loaded vesicles stabilized with cross-linked inner hydrophilic PEG layers exhibited a strong pH-dependent drug release behavior, which can minimize premature drug release during circulation, yet pro-

vide a sufficient drug concentration in a relatively short period of time once internalized by the cancer cells. The DOX and SPIO loading level was 14 and 46 wt %, respectively. The SPIO NPs were dispersed uniformly in the aqueous cores of the vesicles forming a cluster. The high SPIO loading level of the vesicles and the formation of SPIO NP cluster inside the aqueous cores of the vesicles significantly increased the r_2 relaxivity of the SPIO/DOX-loaded vesicles (*i.e.*, 346.1 Fe mM^{-1} s^{-1} *vs* 111.5 Fe mM^{-1} s^{-1} of Feridex) and thus the MRI sensitivity. The FA-conjugated SPIO/DOX-loaded vesicles demonstrated higher cellular uptake and cytotoxicity compared with FA-free vesicles due to folate receptor-mediated endocytosis. Thus, these SPIO/DOX-loaded polymer vesicles offering excellent *in vivo* stability, pH-controlled drug release, and greatly enhanced MRI sensitivity are promising nanomedicine for simultaneous cancer therapy and diagnosis/prognosis.

EXPERIMENTAL METHODS

Reagents and Materials. The heterobifunctional poly(ethylene glycol) (PEG) derivatives, maleimide-PEG_{114}-NH_2 (M_w 5000) and *N*-hydroxysuccinimide-PEG-acrylate (NHS-PEG_{46}-acrylate, M_w 2000), were purchased from JenKem Technology, USA. The anticancer drug, doxorubicin · HCl, was purchased from Tecoland Corporation, USA. γ-Benzyl-L-glutamic acid (BLG), triphosgene, and the fluorescent probes $DiOC_{18}$ and rhodamine B were purchased from Sigma-Aldrich, USA. Folic acid, anhydrous hydrazide, $K_2O_2S_8$, and 2-aminoethanethiol hydrochloride were purchased from Fisher Scientific Inc., USA. All other chemicals used were of analytical reagent grade. Phosphate and acetate buffered solutions were prepared in our laboratory. RPMI-1640 was purchased from Gibco BRL, USA. The human cervical HeLa tumor cell line was purchased from ATCC, USA, and cultured in RPMI medium supplemented with 10% fetal calf serum.

Synthesis of 6 nm Hydrophobic SPIO NPs. Six nanometer hydrophobic SPIO NPs were prepared using the following procedures as reported by Sun *et al.*[45] Briefly, iron(III) acetylacetonate (2 mmol), 1,2-hexadecanediol (10 mmol), oleic acid (6 mmol), oleylamine (6 mmol), and benzyl ether (20 mL) were mixed and magnetically stirred under a flow of nitrogen. The mixture was heated to 200 °C and maintained for 2 h. Then, it was heated to 300 °C to reflux for 1 h. The black-colored mixture was cooled to room temperature by removing the heat source. The black solution was then precipitated with ethanol and separated *via* centrifugation. After discarding the supernatant, the black product was dissolved in hexane in the presence of oleic acid and oleylamine. Centrifugation (6000 rpm, 10 min) was applied to remove the undispersed residue. The product, 6 nm Fe_3O_4 nanoparticles, was then precipitated with ethanol, centrifuged to remove the solvent, and redispersed into hexane.

Preparation of Hydrophilic SPIO NPs. A hexane dispersion of hydrophobic Fe_3O_4 NPs (40 mg in 0.2 mL) was added to a suspension of tetramethylammonium 11-aminoundecanoate in dichloromethane (40 mg in 2 mL). The mixture was shaken using a horizontal laboratory shaker for 24 h. The resulting hydrophilic SPIO NPs were separated using a magnet, washed with dichloromethane, and redispersed in DI water before use.

Synthesis of the Heterofunctional Amphiphilic Triblock Copolymers (FA-PEG_{114}-P(Glu-Hyd-DOX)-PEG_{46}-Acrylate). First, the Mal-PEG_{114}-PBLG copolymers were prepared through ring-opening polymerization of γ-benzyl-L-glutamate *N*-carboxyanhydride (BLG-NCA) using Mal-PEG_{114} (M_w:5000)-NH_2 as a macroinitiator. Typically, 2 g of BLG-NCA was dissolved in 15 mL of anhydrous DMF. After the solution was clear, 100 mg of Mal-PEG_{114}-NH_2 was added into the above solution under stirring. Thereafter, the mixture was stirred at 40 °C for 48 h, after which time the resulting Mal-PEG_{114}-PBLG copolymer was isolated by precipitation in diethyl ether and dried under vacuum. The structure and the number of repeat units of PBLG were evaluated by ^{1}H NMR. Then, FA-PEG_{114}-PBLG copolymer was synthesized *via* a reaction between the thiol group of the thiol-functionalized folate (FA-SH) and the maleimide group of the Mal-PEG_{114}-PBLG copolymer in equal molarity. The reaction was carried out in anhydrous DMF at room temperature for 5 h. Thereafter, the FA-PEG_{114}-PBLG-PEG_{46}-acrylate triblock copolymers were obtained *via* a reaction between the NHS group of NHS-PEG_{46}-acrylate and the distal amino group of FA-PEG_{114}-PBLG. The copolymer was purified by dialyzing against DI water using a cellulose dialysis membrane (MW cutoff = 8000). In order to conjugate DOX onto the hydrophobic segment of the copolymers *via* the acid-sensitive hydrazone bond, the benzyl groups of the FA-PEG_{114}-PBLG-PEG_{46}-acrylate triblock copolymers were substituted with hydrazide by an ester-amide exchange aminolysis reaction. Five hundred milligrams of FA-PEG_{114}-PBLG-PEG_{46}-acrylate was dissolved in 10 mL of anhydrous DMF, and 3 mg of anhydrous hydrazine was added to the solution. The reaction was allowed to proceed at 40 °C at different times to control the degree of benzyl substitution. The resulting FA-PEG_{114}-p(Glu-Hyd)-PEG_{46}-acrylate copolymer was obtained by dialyzing against DI water followed by freeze-drying. After freeze-drying, 200 mg of FA-PEG_{114}-P(Glu-Hyd)-PEG_{46}-acrylate copolymer was dissolved in 10 mL of DMF, and an excess amount (3-fold mol of the copolymers) of DOX · HCl, with respect to the number of DOX binding hydrazide groups conjugated onto the hydrophobic polyglutamate segment of the copolymers, was added. The mixed solution was stirred at room temperature for 24 h while being protected from light. After the reaction was complete, the resulting FA-PEG_{114}-P(Glu-Hyd-DOX)-PEG_{46}-acrylate copolymer was obtained by dialyzing against DI water followed by gel purification using a Sephadex LH-20 column to completely remove any unbound DOX.

FA-free amphiphilic triblock copolymer, methoxy-PEG_{114}-PBLG-PEG_{46}-acrylate, was prepared using methoxy-PEG_{114}-NH_2 as a macroinitiator following the procedures as described above.

Preparation of SPIO/DOX-Loaded Vesicles with Cross-Linked Inner Hydrophilic PEG Layers. Typically, a mixture of 0.009 mg of FA-PEG_{114}-P(Glu-Hyd-DOX)-PEG_{46}-acrylate and 0.291 mg of methoxy-PEG_{114}-P(Glu-Hyd-DOX)-PEG_{46}-acrylate triblock copolymers was dissolved into 5 mL of DI water containing 5 mg of hydrophilic SPIO NPs and 25 μg of $K_2O_2S_8$. The mixture solution was stirred for 5 h followed by sonication for 30 min. The mass ratio between the FA-terminated copolymer and methoxy-terminated copolymer was chosen to ensure a 3% FA molar ratio in the resulting SPIO/DOX-loaded vesicles. After the mixing, the solution was centrifuged to obtain the polymer vesicles with both SPIO NPs and $K_2O_2S_8$ (used as an initiator for the free radical polymerization to cross-link the inner hydrophilic PEG layers *via* the acrylate groups). After discarding the supernatant, the vesicles were resuspended in a water solution. To cross-link the inner hydrophilic PEG layers, the resulting mixture solution was initially bubbled for 30 min with N_2, subsequently heated to 45 °C under N_2, and then stirred for 3 h. After the reaction was complete, the vesicle solution was dialyzed against water to remove the $K_2O_2S_8$. Finally, the solution containing the resulting SPIO/DOX-loaded vesicles with cross-linked inner hydrophilic PEG layers was filtered with a 0.45 μm filter membrane to remove any large aggregates.

Characterization. ^{1}H NMR spectra were recorded on a Bruker DPX 300 spectrometer. Gel permeation chromatography (GPC) analysis was carried out at ambient temperature using the 270max Viscotek (Viscotek, USA) GPC system equipped with triple detectors including a refractive index detector, a viscometer detector, and a light scattering detector. THF was used as an eluent with a flow rate of 1 mL/min. The size and size distribution of the polymer vesicles were determined by dynamic light scattering (DLS) (Malvern Zetasizer Nano Instrument, USA) with an angle detection of 90°. Samples for transmission electron microscopy (TEM, Hitachi H-600, Hitachi, Japan) analysis were pre-

pared by drying a dispersion of the polymer vesicles on a copper grid coated with amorphous carbon. The DOX loading content, defined as the weight percentage of DOX in the polymer vesicles, was quantified by UV−vis analysis using a Varian Cary model 100 Bio UV−vis spectrophotometer. DOX was released from the SPIO/DOX-loaded polymer vesicles in a 0.1 N HCl solution to cleave the hydrazone bonds. The absorbance of DOX at 485 nm was measured to determine the DOX content in the solution using a previously established calibration curve. The DOX loading content measurements were performed in triplicate. The SPIO loading content inside the polymer vesicles was determined using an atomic absorption spectrophotometer (AAS). Briefly, the freeze-dried SPIO/DOX-loaded vesicles were weighed and then added to a 1 M HCl solution to allow complete dissolution of the SPIO NPs. Iron concentration was determined at the specific Fe absorption wavelength (248.3 nm) based on a previously established calibration curve. The SPIO loading content was calculated as the ratio of the weight of encapsulated SPIO NPs to the total weight of the SPIO/DOX-loaded vesicles. The fluorescence intensity of the vesicles containing the fluorescent rhodamine B probes was measured using a FluoroLog-3 modular spectrofluorometer (HORIBA Scientific, USA).

Evaluation of pH-Controlled Drug Release. The pH-responsive DOX release behavior of the SPIO/DOX-loaded vesicles with cross-linked inner hydrophilic PEG layers was studied using a UV spectrophotometer. Briefly, 50 mg of freeze-dried FA-conjugated SPIO/DOX-loaded vesicles (with either cross-linked or non-cross-linked inner PEG layers) was dispersed in 5 mL of medium (phosphate buffer (10 mM, pH 7.4) or acetate buffer (10 mM, pH 5.3)) and was then placed in a dialysis bag with a molecular weight cutoff of 2 kDa. Subsequently, the dialysis bag was immersed in 100 mL of the same medium and kept in a horizontal laboratory shaker maintaining a constant temperature and stirring. At selected time intervals, the buffered solution (5 mL) outside the dialysis bag was removed for UV−vis analysis and replaced by fresh buffered solution with the same volume. The amount of released DOX was analyzed with the UV spectrophotometer at 485 nm. Each sample was measured three times.

Cellular Uptake Study. The cellular uptake behavior and the intracellular distribution of the SPIO/DOX-loaded vesicles were analyzed using both flow cytometry and confocal laser scanning microscopy (CLSM). For flow cytometry, HeLa cells (1×10^6) were seeded in 6-well culture plates and cultured overnight. The cells were then treated with free DOX and FA-conjguated and FA-free SPIO/DOX-loaded vesicles with cross-linked inner hydrophilic PEG layers for 15 and 120 min (DOX concentration 20 μg/mL). Thereafter, the cells were lifted using Cellstripper (Media Tech, Inc., USA) and washed. The DOX uptake was analyzed using a FACSCalibur flow cytometer (BD Bioscience, USA). A minimum of 2×10^4 cells was analyzed from each sample with the DOX fluorescence intensity shown on a four-decade log scale. For CLSM studies, HeLa cells (1×10^6) were seeded onto 22 mm round glass coverslips placed in 6-well plates and cultured overnight. Cells were treated with free DOX and FA-conjugated and FA-free SPIO/DOX-loaded vesicles with cross-linked inner hydrophilic PEG layers for 120 min (DOX concentration = 20 μg/mL). Then, the cells were washed and fixed with 1.5% formaldehyde. Coverslips were placed onto glass microscope slides, and DOX uptake was analyzed using a Leica TCS SP2 confocal system installed on an upright compound microscope (Leica, Wetzler, Germany). Digital monochromatic images were acquired using Leica Confocal Software (version 2.61).

Cytotoxicity Evaluation. The cytotoxicity of the SPIO/DOX-loaded vesicles with cross-linked inner hydrophilic PEG layers against HeLa cells was studied using the MTT assay. First, HeLa cells (1×10^4) were seeded in 96-well plates and incubated for 24 h. The media was replaced with fresh media containing either free DOX or FA-conjugated or FA-free SPIO/DOX-loaded vesicles with cross-linked inner hydrophilic PEG layers at different DOX concentrations or control media and incubated for 48 h. Thereafter, the wells were washed three times with warm phosphate buffer solution and incubated again for another 3 h with RPMI containing 250 μg/mL of MTT. After discarding the culture medium, 200 μL of DMSO was added to dissolve the precipitates and the resulting solution was measured for absorbance at 570 nm with a reference wavelength of 690 nm using a microplate reader (Molecular Devices, USA).

Relaxivity Measurement. All samples were positioned in a Varian (Palo Alto, CA) 7.2 cm inner diameter quadrature coil, and relaxation data were acquired at 4.7 T using a Varian Inova imaging and spectroscopy system. A single slice, multiecho spin echo sequence was used to measure T_2 relaxation times (TR = 8000 ms, TE = 5.75−20.75 ms (16 echoes, 1 s increments), SL = 2 mm, FOV = 60 × 60 mm, MA = 128 × 128). Relaxation times were obtained by fitting the multiecho data to a monoexponential decay curve using linearized least-squares optimization. Relaxivity values were calculated *via* linear least-squares fitting of 1/relaxation time (s^{-1}) *versus* the iron concentration (mM Fe).

Supporting Information Available: Additional supporting figures. This material is available free of charge *via* the Internet at http://pubs.acs.org.

REFERENCES AND NOTES

1. Torchilin, V. P. Multifunctional Nanocarriers. *Adv. Drug Delivery Rev.* **2006**, *58*, 1532–1555.
2. Liong, M.; Lu, J.; Kovochich, M.; Xia, T.; Ruehm, S. G.; Nel, A. E.; Tamanoi, F.; Zink, J. I. Multifunctional Inorganic Nanoparticles for Imaging, Targeting, and Drug Delivery. *ACS Nano* **2008**, *2*, 889–896.
3. Kim, J.; Lee, J. E.; Lee, S. H.; Yu, J. H.; Lee, J. H; Park, T. G.; Hyeon, T. Designed Fabrication of a Multifunctional Polymer Nanomedical Platform for Simultaneous Cancer-Targeted Imaging and Magnetically Guided Drug Delivery. *Adv. Mater.* **2008**, *20*, 478–483.
4. Peer, D.; Karp, J. M.; Hong, S.; Farokhzad, O. C.; Margalit, R.; Langer, R. Nanocarriers as an Emerging Platform for Cancer Therapy. *Nat. Nanotechnol.* **2007**, *2*, 751–760.
5. Zhang, L.; Chan, J. M.; Gu, F. X.; Rhee, J. W.; Wang, A. Z.; Radovic-Moreno, A. F.; Alexis, F.; Langer, R.; Farokhzad, O. C. Self-Assembled Lipid−Polymer Hybrid Nanoparticles: A Robust Drug Delivery Platform. *ACS Nano* **2008**, *2*, 1696–1702.
6. Lu, W.; Arumugam, S. R.; Senapati, D.; Singh, A. K.; Arbneshi, T.; Khan, S. A.; Yu, H.; Ray, P. C. Multifunctional Oval-Shaped Gold-Nanoparticles-Based Selective Detection of Breast Cancer Cells Using Simple Colorimetric and Highly Sensitive Two-Photon Scattering Assay. *ACS Nano* **2010**, *4*, 1739–1749.
7. Heister, E.; Lamprecht, C.; Neves, V.; Tilmaciu, C.; Datas, L.; Flahaut, E.; Soula, B.; Hinterdorfer, P.; Coley, H. M.; Silva, S. R. P.; *et al.* Higher Dispersion Efficacy of Functionalized Carbon Nanotubes in Chemical and Biological Environments. *ACS Nano* **2010**, *4*, 2615–2626.
8. Kim, J.; Park, S.; Lee, J. E.; Jin, S. M.; Lee, J. H.; Lee, I. S.; Yang, I.; Kim, J.-S.; Kim, S. K.; Cho, M.-H.; Hyeon, T. Designed Fabrication of Multifunctional Magnetic Gold Nanoshells and Their Application to Magnetic Resonance Imaging and Photothermal Therapy. *Angew. Chem., Int. Ed.* **2006**, *45*, 7754–7758.
9. Feng, X.; Lv, F.; Liu, L.; Tang, H.; Xing, C.; Yang, Q.; Wang, S. Conjugated Polymer Nanoparticles for Drug Delivery and Imaging. *ACS Appl. Mater. Interfaces* **2010**, *2*, 2429–2435.
10. Rowe, M. D.; Thamm, D. H.; Kraft, S. L.; Boyes, S. G. Polymer-Modified Gadolinium Metal-Organic Framework Nanoparticles Used as Multifunctional Nanomedicines for the Targeted Imaging and Treatment of Cancer. *Biomacromolecules* **2009**, *10*, 983–993.
11. Ai, H.; Flask, C.; Weinberg, B.; Shuai, X.; Pagel, M. D.; Farrell, D.; Duerk, J.; Gao, J. Magnetite-Loaded Polymeric Micelles as Ultrasensitive Magnetic-Resonance Probes. *Adv. Mater.* **2005**, *17*, 1949–1952.
12. Yang, X.; Pilla, S.; Grailer, J. J.; Steeber, D. A.; Gong, S.; Chen, Y.; Chen, G. Tumour-Targeting, Superparamagnetic Polymeric Vesicles as Highly Efficient MRI Contrast Probes. *J. Mater. Chem.* **2009**, *19*, 5812–5817.
13. Sanvicens, N.; Marco, M. P. Multifunctional Nanoparticles-Properties and Prospects for Their Use in Human Medicine. *Trends Biotechnol.* **2008**, *26*, 425–433.

14. Jain, T. K.; Richey, J.; Strand, M.; Pelecky, D. L.; Flask, C.; Labhasetwar, V. Magnetic Nanoparticles with Dual Functional Properties: Drug Delivery and Magnetic Resonance Imaging. *Biomaterials* **2008**, *29*, 4012–4021.
15. Jain, T. K.; Reddy, M. K.; Morales, M. A.; Leslie-Pelechy, D. L.; Labhasetwar, V. Biodistribution, Clearance, and Biocompatibility of Iron Oxide Magentic Nanoparticles in Rats. *Mol. Pharmaceutics* **2008**, *5*, 316–327.
16. Deka, S. R.; Quarta, A.; Corato, R. D.; Falqui, A.; Manna, L.; Cingolani, R.; Pellegrino, T. Acidic pH-Responsive Nanogels as Smart Cargo Systems for the Simultaneous Loading and Release of Short Oligonucleotides and Magnetic Nanoparticles. *Langmuir* **2010**, *26*, 10315–10324.
17. Gaihre, B.; Khil, M. S.; Lee, D. R.; Kim, H. Y. Gelatin-Coated Magnetic Irion Oxide Nanoparticles as Carrier System: Drug Loading and *In Vitro* Drug Release Study. *Int. J. Pharm.* **2009**, *365*, 180–189.
18. Kim, K.; Kim, T. H.; Choi, J. H.; Lee, J. Y.; Hah, S. S.; Yoo, H.-O.; Hwang, S. S.; Ryu, K. N.; Kim, H. J.; Kim, J. Synthesis of pH-Sensitive PEO-Based Block Copolymer and Its Application for the Stabilization of Iron Oxide Nanoparticles. *Macromol. Chem. Phys.* **2010**, *211*, 1127–1136.
19. Peer, D.; Karp, J. M.; Hong, S.; Farokhzad, O. C.; Margalit, R.; Langer, R. Nanocarriers as an Emerging Platform for Cancer Therapy. *Nat. Nanotechnol.* **2007**, *2*, 751–760.
20. Kim, J.; Piao, Y.; Hyeon, T. Multifunctional Nanostructured Materials for Multimodal Imaging, and Simultaneous Imaging and Therapy. *Chem. Soc. Rev.* **2009**, *38*, 372–390.
21. Discher, D. E.; Eisenberg, A. Polymer Vesicles. *Science* **2002**, *297*, 967–973.
22. Antonietti, M.; Förster, S. Vesicle and Liposomes: A Self-Assembly Principle Beyond Lipids. *Adv. Mater.* **2003**, *15*, 1323–1333.
23. Jenecke, S. A.; Chen, L. Self-Assembly of Ordered Microporous Materials from Rod−Coil Block Copolymers. *Science* **1999**, *283*, 372–375.
24. Förster, S.; Antonietti, M. Amphiphilic Block Copolymers in Structure-Controlled Nanomaterial Hybrids. *Adv. Mater.* **1998**, *10*, 195–217.
25. Chécot, F.; Lecommandoux, S.; Gnanou, Y.; Klok, H.-A. Water-Soluble Stimuli-Responsive Vesicles from Peptide-Based Diblock Copolymers. *Angew. Chem., Int. Ed.* **2002**, *41*, 1339–1343.
26. Savic, R.; Azzam, T.; Eisenberg, A.; Maysinger, D. Assessment of the Integrity of Poly(caprolactone)-*b*-Poly(ethylene oxide) Micelles under Biological Conditions: A Fluorogenic-Based Approach. *Langmuir* **2006**, *22*, 3570–3578.
27. Heise, A.; Hedrick, J. L.; Frank, C. W.; Miller, R. D. Starlike Block Copolymers with Amphiphilic Arms as Models for Unimolecular Micelles. *J. Am. Chem. Soc.* **1999**, *121*, 8647–8648.
28. Bae, Y.; Jang, W.-D.; Nishiyama, N.; Fukushima, S.; Kataoka, K. Multifunctional Polymeric Micelles with Folate-Mediated Cancer Cell Targeting and pH-Triggered Drug Releasing Properties for Active Intracellular Drug Delivery. *Mol. Biosyst.* **2005**, *1*, 242–250.
29. Ciuchi, F.; Nicola, G. D.; Franz, H.; Gottarelli, G.; Mariani, P.; Grazia, M.; Bossi, P.; Spada, G. P. Self-Recognition and Self-Assembly of Folic Acid Salts: Columnar Liquid Crystalline Polymorphism and the Column Growth Process. *J. Am. Chem. Soc.* **1994**, *116*, 7064–7071.
30. Prabaharan, M.; Grailer, J. J.; Pilla, S.; Steeber, D. A.; Gong, S. Folate-Conjugated Amphiphilic Hyperbranched Block Copolymers Based on Boltorn H40, Poly(L-lactide) and Poly(ethylene glycol) for Tumor-Targeted Drug Delivery. *Biomaterials* **2009**, *30*, 3009–3019.
31. Luo, L.; Eisenberg, A. Thermodynamic Stabilization Mechanism of Block Copolymer Vesicles. *J. Am. Chem. Soc.* **2001**, *123*, 1012–1013.
32. Du, J.; Tang, Y.; Lewis, A. L.; Armes, S. P. pH-Sensitive Vesicles Based on a Biocompatible Zwitterionic Diblock Copolymer. *J. Am. Chem. Soc.* **2005**, *127*, 17982–17983.
33. Shuai, X.; Merdan, T.; Schaper, A. K.; Xi, F.; Kissel, T. Core-Cross-Linked Polymeric Micelles as Paclitaxel Carriers. *Bioconjugate Chem.* **2004**, *15*, 441–448.
34. Nasongkla, N.; Bey, E.; Ren, J.; Ai, H.; Khemtong, C.; Guthi, J. S.; Chin, S.-F.; Sherry, A. D.; Boothman, D. A.; Gao, J. Multifunctional Polymeric Micelles as Cancer-Targeted, MRI-Ultrasensitive Drug Delivery Systems. *Nano Lett.* **2006**, *6*, 2427–2430.
35. He, J.; Tong, X.; Tremblay, L.; Zhao, Y. Corona-Cross-Linked Polymer Vesicles Displaying a Large and Reversible Temperature-Responsive Volume Transition. *Macromolecules* **2009**, *42*, 7267–7270.
36. Nardin, C.; Hirt, T.; Leukel, J.; Meier, W. Polymerized ABA Triblock Copolymer Vesicles. *Langmuir* **2000**, *16*, 1035–1041.
37. Shuai, X. T.; Ai, H.; Nasongkla, N.; Kim, S. J.; Gao, J. M. Micellar Carrier Based on Block Copolymers of Poly(ε-caprolactone) and Poly(ethylene glycol) for Doxorubicin Delivery. *J. Controlled Release* **2004**, *98*, 415–426.
38. Prabaharan, M.; Grailer, J. J.; Pilla, S.; Steeber, D. A.; Gong, S. Q. Gold Nanoparticles with a Monolayer of Doxorubicin-Conjugated Amphiphilic Block Copolymer for Tumor-Targeted Drug Delivery. *Biomaterials* **2009**, *30*, 6065–6075.
39. Lee, Y.; Park, S. Y.; Mok, H.; Park, T. G. Synthesis, Characterization, Antitumor Activity of Pluronic Mimicking Copolymer Micelles Conjugated with Doxorubicin *via* Acid-Cleavable Linkage. *Bioconjugate Chem.* **2008**, *19*, 525–531.
40. Rohrer, M.; Bauer, H.; Mintorovitch, J.; Requardt, M.; Weinmann, H. J. Comparison of Magnetic Properties of MRI Contrast Media Solutions at Different Magnetic Field Strengths. *Invest. Radiol.* **2005**, *40*, 715–724.
41. Russier, V.; Petit, C.; Pileni, M. P. Hysteresis Curve of Magnetic Nanocrytals Monolayers: Influence of the Structure. *J. Appl. Phys.* **2003**, *93*, 10001–10010.
42. Lim, Y. T.; Noh, Y.-W.; Han, J. H.; Cai, Q.-Y.; Yoon, K.-H.; Chung, B. H. Biocompatible Polymer-Nanoparticles-Based Bimodal Imaging Contrast Agents for the Labeling and Tracking of Dendritic Cells. *Small* **2008**, *4*, 1640–1645.
43. Taboada, E.; Solanas, R.; Rodriguez, E.; Weissleder, R.; Roig, A. Supercritical Fluid-Assisted One-Pot Synthesis of Biocompatible Core(γ-Fe_2O_3)/Shell(SiO_2) Nanoparticles as High Relaxivity T_2-Contrast Agents for Magnetic Resonance Imaging. *Adv. Funct. Mater.* **2009**, *19*, 2319–2324.
44. Kim, J.; Piao, Y.; Hyeon, T. Multifunctional Nanostructured Materials for Multimodal Imaing, and Simultaneous Imaging and Therapy. *Chem. Soc. Rev.* **2009**, *38*, 372–390.
45. Sun, S.; Zeng, H.; Robinson, D. B.; Ranous, S.; Rice, P. M.; Wang, S.; Li, G. Monodisperse MFe_2O_4 (M = Fe, Co, Mn) Nanoparticles. *J. Am. Chem. Soc.* **2004**, *126*, 273–279.